Polymer Chemistry

Accepted Manuscript

ROYAL SOCIETY OF CHEMISTRY

www.rsc.org/polymers

Using click chemistry to dial up the modulus of doubly crosslinked microgels through precise control of microgel building block functionalisation

Robert Farley[a], Silvia Halacheva[b], Jane Bramhill[c] and Brian R. Saunders[a,*]

[a] *Biomaterials Research Group, Manchester Materials Science Centre, School of Materials, The University of Manchester, Grosvenor Street, Manchester, M1 7HS, U.K.*

[b] *University of Bolton, Institute for Materials Research and Innovation, Deane Road, Bolton, Greater Manchester, BL3 5AB, U.K.*

[c] *Gelexir Healthcare Ltd, C/O- UMI3 CTF, 46 Grafton Street, Manchester, M13 9NT, U.K.*

ABSTRACT:

Doubly crosslinked microgels (DX MGs) are hydrogels constructed by covalently interlinked vinyl-functionalised microgel particles. Until now it has not been possible to precisely control the extent of vinyl functionalisation of the microgel (MG) particles which act as the colloidal building blocks for hydrogel assembly. Furthermore, the range of DX MGs prepared to date has been modest. This study addresses both of these challenges by constructing a new class of DX MG using MG particles that were vinyl functionalised by copper catalysed azide-alkyne cycloaddition (CuAAC). Here, poly(2-vinylpyridine-*co*-propargyl acrylate) (PVP-PA) MG particles were prepared and vinyl functionalised by CuAAC using azidopropyl methacrylate (AZPMA) to give PVP-PA$_x$-PMA$_y$ MGs. Values for the extent of vinyl functionalisation (y) were varied from 0 to 7.0 mol.% in a precisely controlled manner. Concentrated dispersions were transformed from fluids to physical gels at pH values of less than or equal to 3.0 and covalently inter-linked to give PVP-PA$_x$-PMA$_y$ DX MGs by free-radical coupling of the vinyl groups of neighbouring particles. The storage modulus of the DX MGs varied linearly with both MG concentration and the value for y. Not only did the new DX MGs studied here enable precise control of MG functionalisation

and DX MG mechanical properties, they also showed evidence of colloidal crystallinity which may lead to future photonic gel applications. Our CuAAC-based approach should be versatile and is expected to enable a range of new DX MGs to be prepared.

INTRODUCTION

Hydrogels continue to attract major attention in the literature with advances in structure-property relationships increasing the opportunities for application[1-3]. Not only have the mechanical properties such as ductility and toughness improved greatly[1, 2] but the ability to design next generation gels with increasingly sophisticated structure-function relationships has rapidly evolved[4-6]. The latter has been enabled by a range of new chemistries which are well suited to hydrogel construction, such as highly efficient copper catalysed azide-alkyne cycloaddition (CuAAC)[7, 8]. Hydrogels with tunable nanomorphologies are a subgroup of next generation hydrogels that hold great promise. A new approach for construction of hydrogels using covalent inter-linking of swellable microgel (MG) particles has recently emerged[9]. MG particles are crosslinked polymer colloid particles that swell when the pH approaches the pK_a of the constituent polymer[10]. MG particles are singly crosslinked (SX) via intra-particle crosslinking and are termed SX MGs. Concentrated dispersions of swollen SX MGs can be covalently inter-linked to form doubly crosslinked MGs (DX MGs[11]). The MG particles are colloidal building blocks for DX MG hydrogels. A key requirement for enabling DX MG construction from MGs is vinyl functionalisation of the MG particle peripheries. However, until now this approach has required use of relatively low efficiency functionalisation chemistry[9, 12] which has been limited to MG particles containing carboxylic acids[9] or primary amines[12]. Building on CuAAC chemistry and our earlier study with MG particles containing propargyl acrylate (PA)[13] we aimed to establish a new family of DX MGs with well-controlled vinyl functionalisation. We hypothesised that the DX MG modulus could be tuned precisely by vinyl group functionalisation. Because the CuAAC approach is versatile[8] this study should expand the range of DX MGs that can be prepared and investigated.

The overwhelming majority of hydrogel research involves network construction using small molecules, i.e., monomers[14, 15]. By contrast DX MGs contain pre-formed colloidal scale gel particles which enable design of gel nanomorphology on the length scale of ~ 50 to 1000 nm and may provide new photonic and biomaterial hydrogels. A key challenge for achieving improved DX MGs is the ability to vary the vinyl functionalising extent of MG particles in a precise manner that is also versatile. The present study addresses these challenges by establishing a new method for the vinyl functionalisation of MG particles and using this to construct new DX MGs. For this study we used MGs based on poly(2-vinyl pyridine) (PVP), which exhibit strong pH-triggered swelling. PVP particles swell when the pH decreases to below the pK_a, which is about 4.9[16]. Whilst PVP MGs have been studied by a number of groups[16-18] they have not been reported in the context of DX MG formation until now.

Click chemistry was pioneered by Sharpless et al.[19] and has proven to be an exceptionally efficient and versatile functionalisation approach for polymers, particles, beads[20] and surfaces[8, 21]. CuAAC has also been used to prepare a new range of hydrogels by playing an integral role in the network formation process[4, 22]. By contrast to those studies the present work uses CuAAC to functionalise pre-formed MG particles, which are subsequently inter-linked to form hydrogels. Whilst CuAAC has also been explored in the context of MG particle functionalisation[13, 23, 24], it has not yet been reported in the context of vinyl functionalisation of MGs to the best of our knowledge.

Previously,[13] we investigated PVP-PA MG particles and showed that they could be functionalised with primary amines via CuAAC using 2-azido-1-ethylamine. The MG particle functionalisation was highly efficient and the MG particles retained their strong pH-dependent swelling. Building on our earlier study[13] we hypothesised that high efficiency vinyl functionalisation of PVP-PA MGs could be achieved using a methacrylated azide. For this study we used azido propyl

methacrylate (AZPMA) – See Scheme 1a. In our approach PVP-PA MG particles containing a small proportion of crosslinker (divinyl benzene) were functionalised with AZPMA via CuAAC. Concentrated PVP-PA$_x$-PMA$_y$ MG dispersions containing α,α'-azodiisobutyramidine dihydrochloride (AIBA) were subsequently swollen at pH = 3 to form physical gels and then covalently crosslinked using free-radical coupling to give PVP-PA$_x$-PMA$_y$ DX MGs (Scheme 1b).

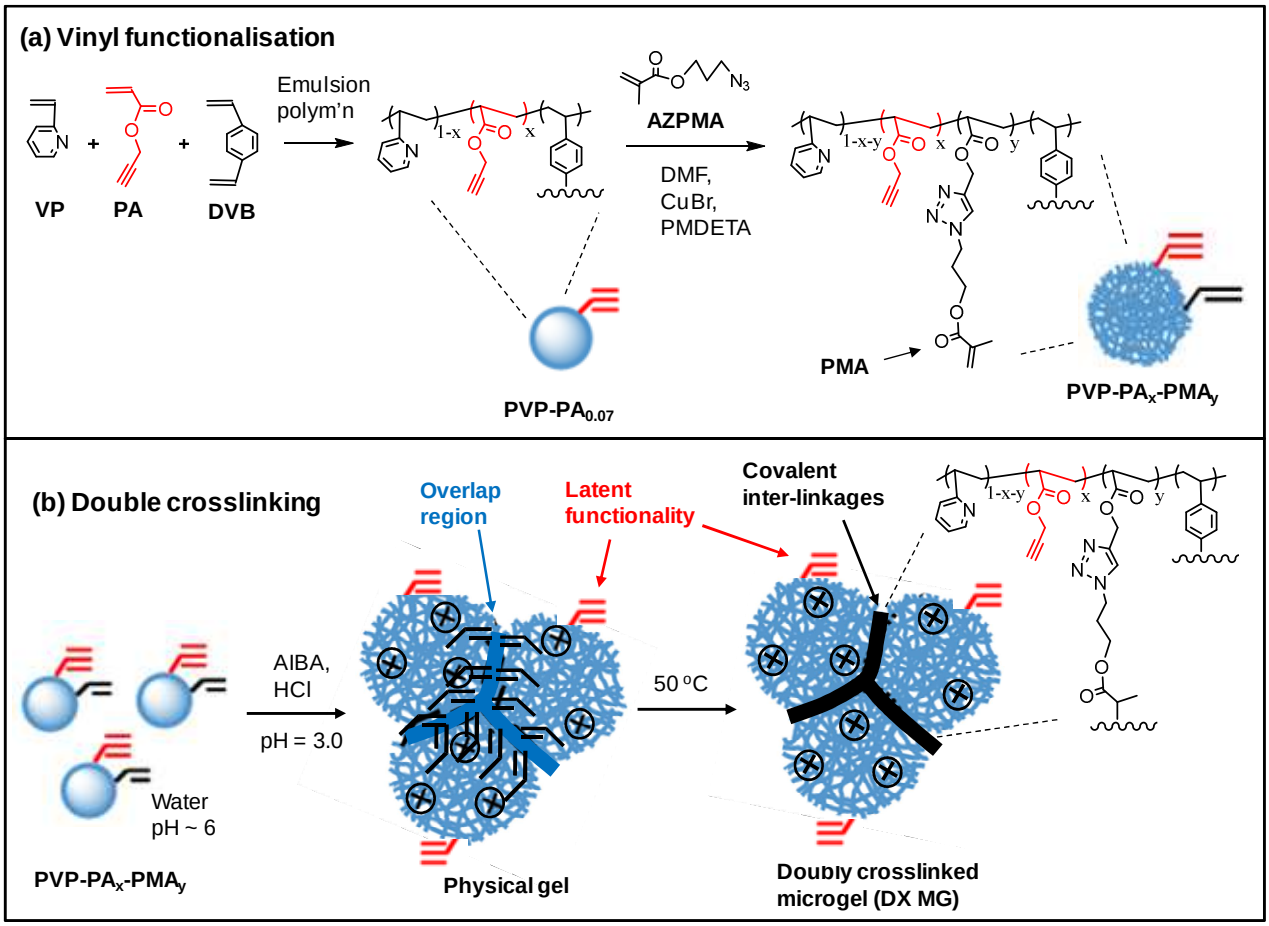

Scheme 1. Depiction of synthesis of PVP-based DX MGs from vinyl functionalised MGs. (a) Vinyl functionalisation via CuAAC was conducted using PVP-PA MG particles synthesised by emulsion polymerisation. (b) DX MGs were formed after pH-triggered swelling of the PVP-PA$_x$-PMA$_y$ MG particles caused overlap of the peripheries which enabled covalent inter-linking of the MG particles by free-radical coupling.

In this report we first determine the compositions of PVP-PA$_x$-PMA$_y$ MG particles using a combination of elemental analysis and FTIR to quantify the extents of vinyl functionalisation. Photon correlation spectroscopy and electrophoretic mobility measurements are also used to probe the pH-dependence of the hydrodynamic diameter and zeta potential of the MG particles. The morphologies of the DX MGs is then investigated using SEM and the mechanical properties studied using dynamic rheology. The data show that the modulus of the DX MGs can be precisely

controlled by MG concentration and the extent of PMA incorporation. The results show that CuAAC is a highly efficient and versatile method for obtaining DX MGs with modulus values that can be controlled precisely. The results of this study should enable a wide range of new DX MGs to be prepared.

EXPERIMENTAL

Materials

2-Vinyl pyridine (VP, 97%), propargyl acrylate (PA, 98%), divinylbenzene (DVB, 80%), α,α'-azodiisobutyramidine dihydrochloride (AIBA, 97%), 3-chloro-1-propanol (98%), sodium azide ($\geq$ 99%), methacryloyl chloride ($\geq$ 97%), hydroquinone, anhydrous dichloromethane ($\geq$ 99.8%), trimethylamine ($\geq$ 99%) and tetrabutylammonium hydrogen sulphate (97%) were all purchased from Sigma-Aldrich and used as received unless otherwise stated. PVP MG was prepared following the method reported previously[13]. VP and PA were purified by passing them through columns packed with basic alumina. High purity distilled, deionised water was used for all experiments.

Synthesis of 3-azidopropyl methacrylate

Azidopropyl methacrylate (AZPMa) was synthesised in accordance with the literature[25]. Briefly, 3-chloro-1-propanol (33.9 g, 0.36 mol) was introduced to a mixture of sodium azide (47 g, 0.72 mol), tetrabutylammonium hydrogen sulphate (1.0 g, 2.95 mmol) and water (40 mL). The slurry was heated to 80 °C for 24 h whilst stirring. After cooling to room temperature, stirring was continued for a further 14 h. Following an ether extraction the resulting solution was dried over anhydrous sodium sulphate and the solvent removed under reduced pressure. Vacuum distillation was employed to obtain 3-azidopropanol (AZPOH). The purity of AZPOH was verified by ^{1}H NMR. Then AZPOH (23.5 mL, 0.253 mol), dried triethylamine (45 mL, 0.323 mol), hydroquinone (0.1 g) and dried dichloromethame (100 mL) were combined under stirring and

cooled in an ice / water bath. Whilst maintaining a constant temperature of 0 °C, methacryloyl chloride (29 mL, 0.3 mol) was slowly added dropwise over a period of 20 min. Stirring was continued at 0 °C for 1 h and then for a further 14 h at room temperature. An additional 100 mL of dichloromethane was added before the mixture was extracted with aqueous HCl (0.3 M), followed by water, then aqueous NaOH (2.5 M) and a further water extraction step. Each extraction step listed was conducted twice. Hydroquinone (0.1 g) was added to the resultant solution, which was then dried. The solvent was removed using rotary evaporation to yield AZPMa. The ^{1}H NMR spectrum for AZPMA is shown in Fig. S1 (†, ESI) and is consistent with high purity.

Synthesis of PVP-PA MG

The PVP-PA MG was synthesised by emulsion polymerisation using a modification of the method previously employed[13]. The PA concentration used in this study was much lower than in previous work[13]. Briefly, Aliquat 336 surfactant (1.5 g) and PEGMA2000 (1.5 g) were dissolved in deionised water (120 mL). The solution was transferred to a reaction vessel fitted with an overhead stirrer, heated to 60 °C and degassed with nitrogen. A co-monomer solution of VP (10.72 g, 0.102 mol.), PA (2.18 g, 0.020 mol.) and DVB (0.096 g, 0.74 mmol.) was introduced with stirring at 250 rpm followed by addition of AIBA initiator (0.15 g in 15 mL of water). The emulsion polymerisation was continued for 24 h, before heating was stopped and the dispersion purified by repetitive centrifugation and redispersion in water. Elemental analysis showed that the MG particles contained 7.3 mol.% of PA (See Table 1 and Table S1 (†, ESI)).

Table 1. Compositions of the microgels prepared for this study.

Code	Composition	$R_{NC(exp)}$ [a]	y_{thr} [b]	y_{exp} [c]	%Click [d]	d_{SEM} [e] / nm	$d_{h(3)}$ [f] / nm	$d_{h(7)}$ [f] / nm	Q [g]	ζ [h] / mV
P-0	PVP-$PA_{0.07}$	0.147	0	0	-	315 (9.5)	1315	370	45	33.0
P-1	PVP-$PA_{0.05}$-$PMA_{0.02}$	0.152	0.020	0.016	79.5	300 (7.2)	1375	355	58	34.2
P-2	PVP-$PA_{0.04}$-$PMA_{0.03}$	0.157	0.040	0.029	73.0	325 (8.4)	1475	345	80	31.1
P-3	PVP-$PA_{0.02}$-$PMA_{0.05}$	0.165	0.060	0.053	89.5	325 (8.4)	1380	340	67	33.2
P-4	PVP-$PMA_{0.07}$	0.170	0.073	0.070	96.0	330 (7.0)	1375	345	64	33.8

[a] Ratio of %N to %C determined from elemental analysis data. The latter values together with the uncertainties are given in Table S1 (†, ESI). [b] Theoretical y value based on the molar ratios of reactants used. [c] Experimental y value determined from $R_{NC(exp)}$ (See text). [d] %Click = 100 x (y_{exp} / y_{thr}). [e] Number-average diameter determined from SEM. The numbers in brackets are the coefficient of variation. [f] Hydrodynamic diameter measured at pH = 3 or 7. [g] Volume-swelling ratio at pH = 3, i.e., $Q = (d_{h(3)}/ d_{h(7)})^3$. [h] Zeta potential measured at pH = 3.0.

Synthesis of PVP-PA_x-PMA_y microgels using CuAAC

The method used for preparing each PVP-PA_x-PMA_y MG (Scheme 1) differed only in the amount of AZPMA added. The following gives an example for the preparation of P-1 (Table 1). A concentrated PVP-PA MG dispersion containing 1.0 g of polymer was redispersed in DMF (20 mL) and transferred to a 50 mL Schlenk flask. AZPMa (0.032 g, 0.19 mmol) and PMDETA (0.0165 g, 0.095 mmol) were added and the solution subjected to successive freeze-pump-thaw cycles before an Ar atmosphere was introduced. CuBr (0.0136 g, 0.095 mmol) was added and the solution stirred for 16 h under Ar at room temperature. The resultant MG dispersion was purified by extensive centrifugation and redispersion in water. The method was repeated to prepare P-2 to P-4 (Table 1) using proportional scaled quantities of AZPMa. For example, the mass of AZPMA used for P-3 was 0.096 g (0.57 mmol).

Synthesis of DX MG gels

The MG dispersions (pH ~ 6) were concentrated to 10 wt% using centrifugation (6000 rpm). AIBA (9.0 mg, 0.033 mmol) was added to the MG dispersion (1.5 g) which was then thoroughly mixed using a vortex mixer. The pH of the dispersion was decreased to 3.0 by addition of aqueous HCl (4 M) to trigger physical gel formation. The physical gels were placed in O-rings (20 mm

diameter, 2 mm wall thickness) between glass plates, which were then sealed. The assembly was placed in an oven at 50 °C for 12 h.

Physical Measurements

Elemental analysis of microgels (C, H and N) was performed with a Thermo Scientific Flash 2000 Elemental Analyzer instrument. The standards used for calibration were acetanilide and 2,4 dinitrophenylhydrazone and MG samples were freeze-dried prior to analysis. Proton nuclear magnetic resonance (^{1}H NMR) spectroscopy measurements were conducted on a Bruker 400 Hz instrument with deuterated chloroform used as the solvent. FTIR spectroscopy analysis was carried out using a Nicolet 5700 ATR FTIR apparatus. MG samples were freeze-dried prior to FTIR analysis. Photon correlation spectroscopy (PCS) measurements were performed using a Brookhaven BI-9000 light scattering instrument containing a 20 mW HeNe laser using a scattering angle of 90^o. The electrophoretic mobilities of MG particles were recorded in the presence of aqueous $NaNO_3$ (0.001 M) using a Malvern Zetasizer. The mobilities were converted to zeta potentials (ζ) using the Smoluchowski equation[26]. SEM images were obtained using a Philips XL30 FEGSEM apparatus. Dilute MG dispersions were dried onto glass slides at room temperature. The hydrogel samples were freeze-dried for SEM analysis. All samples were coated with Au or Pd. A minimum of 100 particles were measured to calculate the number-average particle diameter. Dynamic rheology measurements were performed using a TA Instruments AR G2 temperature-controlled rheometer with an environmental chamber. A 20 mm diameter plate geometry with a solvent trap was used. A strain of 1 % was used for the frequency-sweep measurements.

RESULTS AND DISCUSSION

Preparation of microgel particles with precise extents of vinyl functionalisation

Scheme 1 shows the reaction scheme use to prepare the PVP-$PA_{0.07}$ MG particles. Our earlier work established that PVP-PA MGs containing high PA contents (~ 18 mol.%) contained intra-particle crosslinking due to PA coupling[13]. In this study we wanted to promote pH-triggered particle swelling to maximise contact between neighbouring particles in the physical gel state and subsequent crosslinking of peripheral vinyl groups to form DX MGs. Consequently, we used a much lower PA content (~ 7 mol.%). As will be shown below this MG composition provided strong pH-triggered swelling and enabled formation of a range of DX MGs.

Elemental analysis is a powerful method for determining the extent of functionalisation of PA groups within PVP-PA MGs[13]. The high sensitivity of this approach relies on the rapid change of the ratio of the %N to %C values with MG functionalisation. Experimental values for the %N to %C ratio ($R_{NC(exp)}$ = %N/%C) were calculated and are plotted against the theoretical extent of vinyl functionalisation (i.e., y_{thr}) in Fig. 1a. A linear increase of $R_{NC(exp)}$) with y_{thr} is evident which is strong support for the success of CuAAC for vinyl functionalisation (Scheme 1).

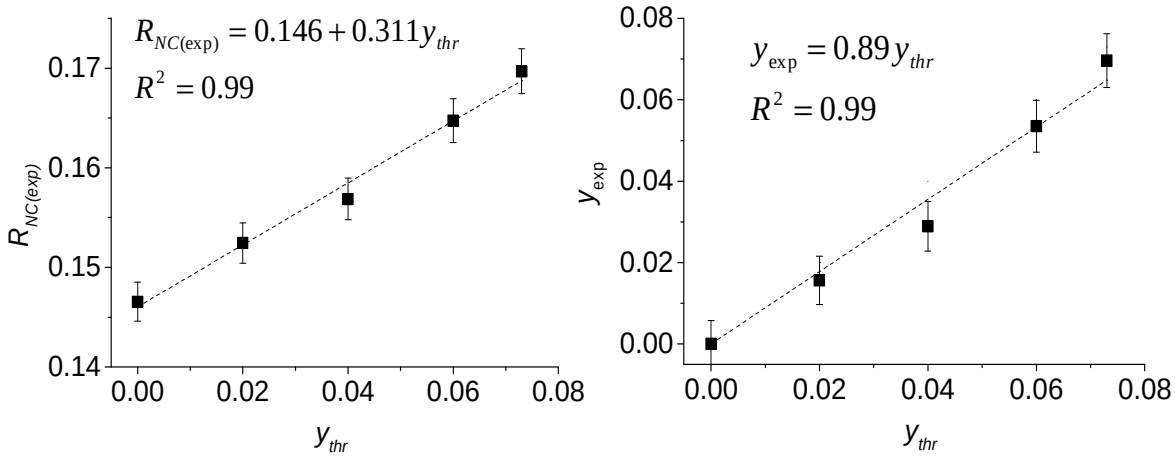

Fig. 1. Microgel composition analysis using elemental analysis data. (a) The variation of $R_{NC(exp)}$ (= %N/%C) with the theoretical *y* value determined from the masses of reactants used for CuAAC. (b) Dependence of the experimentally determined *y* value with the theoretical *y* value for the MG particles.

Building on earlier work[13] we used values for $R_{NC(exp)}$ to calculate experimental *y* values (y_{exp}). The method, general formulae and equations employed are described in the Supplementary Information (†, ESI). Fig. 1b shows that a linear relationship between y_{exp} and y_{thr} occurred with a gradient close to unity. The efficiency of the click reactions (%Click = 100 x y_{exp} / y_{thr}) was calculated (Table 1) and found to be between 73 and 96 %. These high values imply that the MG particles were sufficiently swollen by DMF to allow extensive permeation of the MG interior by the reactants (AZPMA, CuBr and PMDETA). Moreover, these data indicate high click conversion efficiencies were achieved. This finding agrees with our earlier work for related MGs[13].

To further probe the compositions of the PVP-PA_x-PMA_x particles we used FTIR spectroscopy. Spectra for these MGs as well as PA, PVP and AZPMA over the 500 – 4000 cm^{-1} range are shown in Fig. S3 (†, ESI). The spectra for the PVP-PA_x-PMA_y MGs show the presence of PVP bands in the 1000 – 1600 cm^{-1} region as well as PA signals in the region of 1730 cm^{-1} which are discussed below. The spectra do *not* show evidence of the azide band at[27] 2100 cm^{-1}, which was present for AZPMA. The lack of the azide band supports the view that efficient CuAAC occurred. A weak (observable) band due to C=C was present at 1635 cm^{-1} in the spectra for the P-1 to P-4 copolymers (see inset of Fig. S3) and was most pronounced for P-4, as expected. This band provides direct confirmation of vinyl functionalisation of the PVP-PA_x-PMA_y MG particles.

The C=O bands in the 1715 – 1735 cm^{-1} region of the PVP-PA_x-PMA_y spectra were sensitive to the *y* value. Expanded views of the FTIR spectra are shown in Fig. 2a. The C=O bands for the PA and PMA species had different stretching frequencies; i.e., 1715 cm^{-1} for PMA and 1735 cm^{-1} for PA. These differences are ascribed to different distances of the C=O groups to the triazole ring for each moiety (structures shown in Scheme 1). It can be seen from Fig. 2a that the relative absorbance of the C=O bond due to PMA (C=O(PMA)) increased as y_{exp} increased from 0 (for P-0) to 0.07 (for P-4). We explored the latter trend by calculating $A^{Corr}_{N(1715)}$ which is the absorbance

of the 1715 cm^{-1} band due to PMA (A_{1715}) normalised to that of the 1590 cm^{-1} band due to the C=N of the pyridine ring[28] (A_{1590}).

$$A^{Corr}_{N(1715)} = \frac{A_{(1715)}}{A_{(1590)}} - \frac{A^{P-0}_{(1715)}}{A_{(1590)}} \qquad (1)$$

The second term on the right hand side is a correction for the P-0 signal which contributes to the signal for the PMA C=O in the other spectra. The values for eq. (1) are plotted as a function of y_{exp} in Fig. 2b. Good linearity is evident which supports the view that the PMA content increased in proportion with y_{exp}. These data support the elemental analysis performed above and confirm our proposal that efficient CuAAC occurred during the vinyl functionalisation of the PVA-PA MG particles by AZPMA.

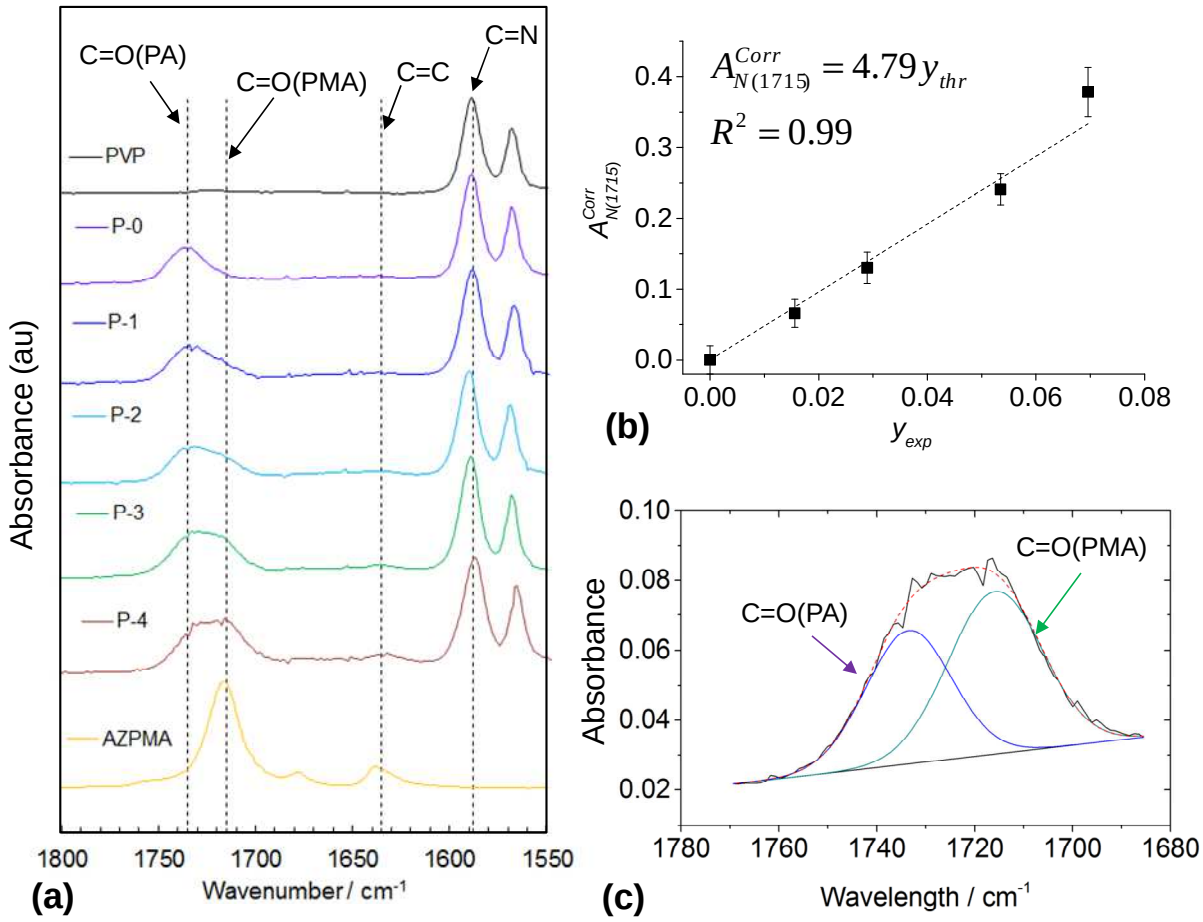

Fig. 2 FTIR investigation of vinyl functionalisation of PVP-PA$_x$-PMA$_y$ MG particles. (a) FTIR spectra for each of the MG systems studied. Data for PVP and AZPMA are shown for comparison. (b) Variation of $A^{Corr}_{N(1715)}$ with y_{exp} – see text. (c) Deconvoluted C=O band for P-4.

The P-4 MG particles contained the highest PMA content and the spectrum for the C=O region

was most suitable for deconvolution (Fig 2c). Deconvolution of the bands due to PMA and PA gave a PMA mole fraction of 0.57, which corresponds to $y = 0.083$. By comparison the y_{exp} value was 0.070 (Table 1) with an error of ± 0.007 (Table S1, †, ESI). The difference between these values is not considered significant. These data, taken together with the linearity from Fig. 2b, support the elemental analysis data (Fig. 1). Accordingly, we propose that it is straightforward to *dial up* the vinyl functionalisation extent of MG particles using CuAAC. More generally, based on the present study and our previous work using different azide species[13], the approach used here should enable further or alternative functionalisation of these PA-containing MG particles in a controllable manner.

Vinyl-functionalised microgel particle properties

The PVP-PA_x-PMA_y MG particles were characterised using SEM (Fig. 3a/b and Fig. S4) and had coefficients of variation (Table 1) less than 10%. The MG particles were monodisperse. At pH values greater than or equal to 4.0 the MG particles were in the collapsed state with the average hydrodynamic diameters for the PVP-PA_x-PMA_y MG particles in the range 340 - 355 nm. It can be seen from Table 1 that there was reasonable agreement between hydrodynamic diameters at pH = 7 ($d_{h(7)}$) and number-average SEM diameters with the former only slightly larger than the latter. We conclude that our CuAAC method for vinyl functionalising PVP-PA MG particles did not compromise colloidal stability, which is highly desirable for a functionalisation approach.

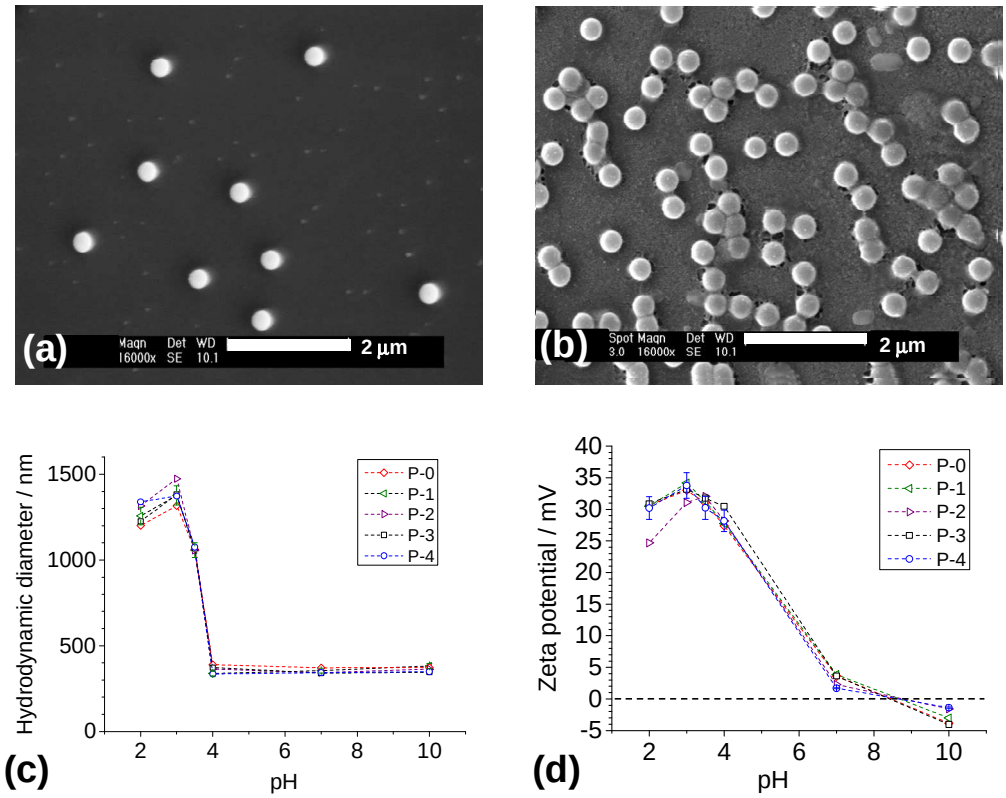

Fig. 3 Properties of PVP-PA-PMA microgel particles. (a) and (b) show representative SEM images for P-0 and P-4 particles, respectively. (c) and (d) show PCS and zeta potential data, respectively, for a range of pH values.

In all cases the MG particles exhibited strong swelling with high volume-swelling ratios (Q) in the range 45 to 80 (Table 1). These Q values are much higher than the Q value of 3.3 reported for the PVP-PA MG particles studied earlier[13]. The latter system contained more than twice the PA content compared to the PVP-$PA_{0.07}$ MGs employed here. The high Q values obtained in this study support the view that intra-particle crosslinking due to PA coupling and / or hydrophobic association, was not significant. The concentrated PVP-PA_x-PMA_y dispersions were well suited to pH-triggered physical gel formation, and hence inter-MG linking to form DX MGs, because PMA functionalisation did not restrict particle swelling at low pH (Fig. 3c).

The pH-dependent zeta potential (ζ) data (Fig. 3d) show that the MG particles were positively charged at pH values less than or equal to 7.0 and generally agree with earlier reports for PVP-based MG particles[13, 16]. We note that microgel electrokinetic data are often reported in terms of electrophoretic mobility and this distinction originates in large part from the pioneering work of Ohshima et al., which has recently been reviewed elsewhere[29]. Here, ζ values are shown to

facilitate comparison with the earlier studies[13, 16]. CuAAC did not significantly affect the ζ values. Furthermore, the latter values were not significantly affected by y_{exp}. This result is not surprising because at low pH the MG particles had a very high positive volume-charge density and functionalisation should not extinguish charge because it provides charged triazole groups. It also follows from these data that DX MGs prepared in this study from the PVP-PA_x-PMA_y MGs (below) were cationic.

Synthesis and morphology of doubly crosslinked microgels

The DX MG formation process involved triggered physical gel formation (Fig. 4a) and covalent interlinking of the particles to form a permanent gel (Scheme 1). Physical gels formed when the MG concentration was greater than or equal to 5 wt.% and pH less than 4.0. In the physically gel state the MG particle peripheries overlap and covalent crosslinking can occur. Generally, the DX MGs had good transparency (Fig. 4d), which is due to the high extents of swelling of the constituent MG particles.

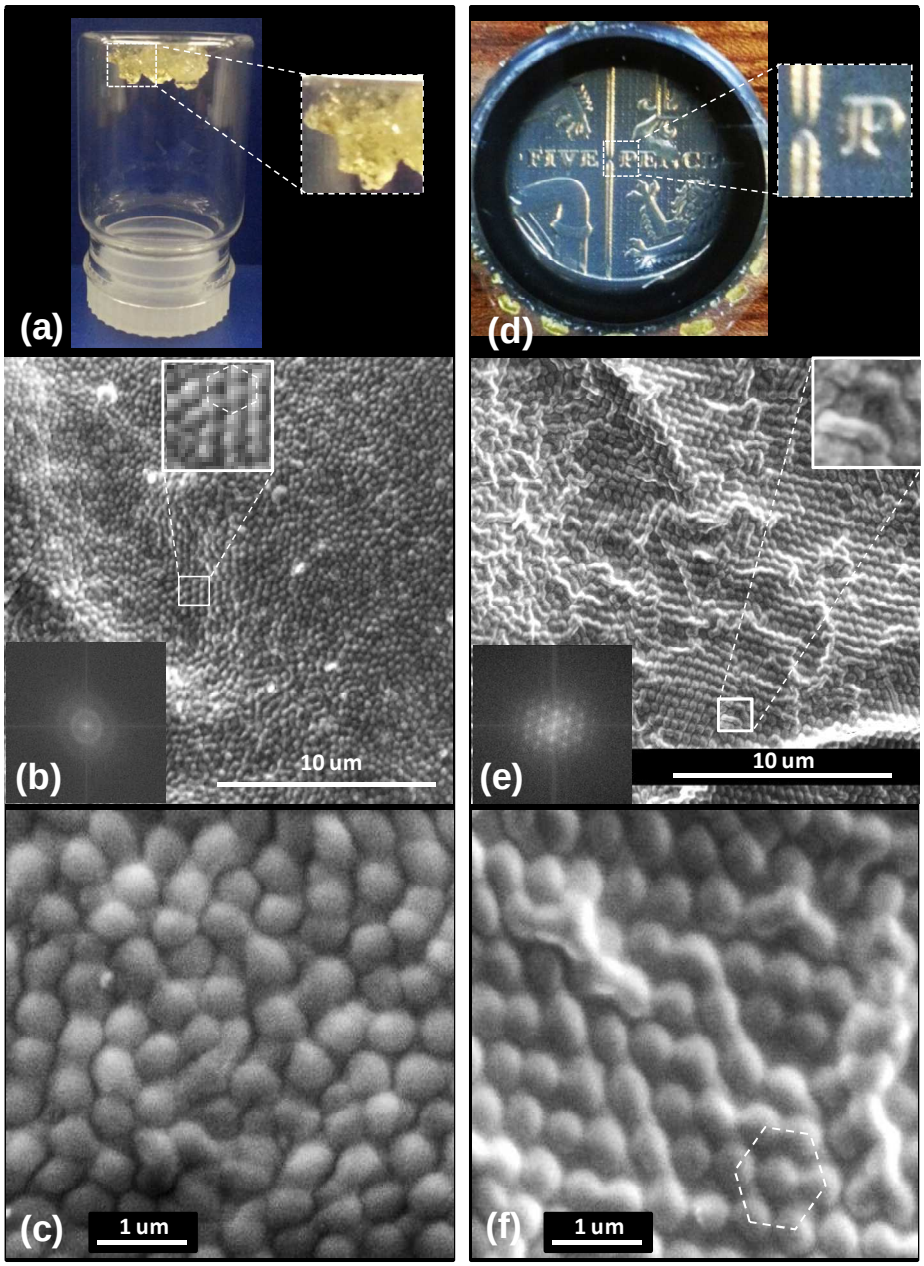

Fig. 4. **Morphologies of physical and covalent P-2 gels.** Physical SX MG gels are shown on the left hand side and covalent DX MG gels are shown on the right hand side. Digital photographs of the gels are shown in (a) and (d). Representative SEM images appear in (b), (c), (e) and (f). The thickness of the DX MG shown in (d) was 2 mm. The insets for (b) and (e) are Fast Fourier Transform images of the micrographs.

We probed the morphologies of freeze-dried SX MG physical gels and DX MG covalent gels using SEM (Fig. 4b, c, e and f). SEM images for P-2 gels before (b and c) and after (e and f) DX MG formation are shown. MG particles are clearly evident which shows that they maintained their integrity upon macroscopic gel formation. The SEM images showed the MG particle packing was mostly disordered for the physical gel (Fig. 4b and c). Interestingly, a mostly crystalline arrangement was evident for the DX MG (Fig. 4e and f). However, close examination of the SEM

images (insets for Fig. 4b and e) showed there were some domains with the opposing morphologies present for each system, i.e. ordered assembly for the mostly disordered physical gel (Fig. 4b) and disordered for the mostly ordered DX MG (Fig. 4e).

Fast Fourier Transform (FFT) images (see insets of Fig. 4b and e) confirmed that amorphous and crystalline morphologies were dominant for the physical SX MGs and covalent DX MGs, respectively. The physical gel showed amorphous halos; whereas, the DX MG showed an hexagonal array of points. (These differences were repeatable for different domains within the samples.) It is interesting to note that recently reported polyvinylamine DX MGs were also reported to have crystalline order[12]. It is suggested that crystalline order is favoured for DX MGs comprised of MG particles with low size polydispersity. It is the control (and locking in) of ordered particle arrangements with spacings comparable to the wavelength of light that may allow DX MGs to be prepared for new photonic applications. Furthermore, if the interstitial sites apparent in Fig. 4e and f act as pores these new DX MGs may have potential application as membranes. These aspects will be explored in future work.

Dialing up doubly crosslinked microgel modulus

Having established that functionalisation of the MG particles could be precisely controlled we next sought to investigate the ability to control DX MG mechanical properties. We first examined the effect of MG concentration (C_{MG}) on the dynamic rheological properties. The P-2 system was selected for this study because of its good combination of optical clarity (Fig. 4d) and ordered morphology (Fig. 4f).

Frequency-sweep dynamic rheology measurements were obtained for P-2 gels prepared using a range of C_{MG} values and are shown in Fig. 5a and b. The *G'* (storage modulus) values had very low frequency dependence and the gels exhibited solid-like viscoelastic behaviour. The latter is a common feature reported for DX MGs[12, 30]. The tan δ values (= *G"*/*G'*) were less than 0.10 (Fig.

5b) which shows that the gels were mostly elastic. Whilst most of the DX MGs had frequency dependent tan δ values, the data obtained using C_{MG} = 10% had negligible frequency dependence. Winter and Chambon[31] established that systems at the critical gel points have frequency independent tan δ values. It follows that the DX MG prepared using C_{MG} = 10% exhibited critical behaviour over the frequency region studied.

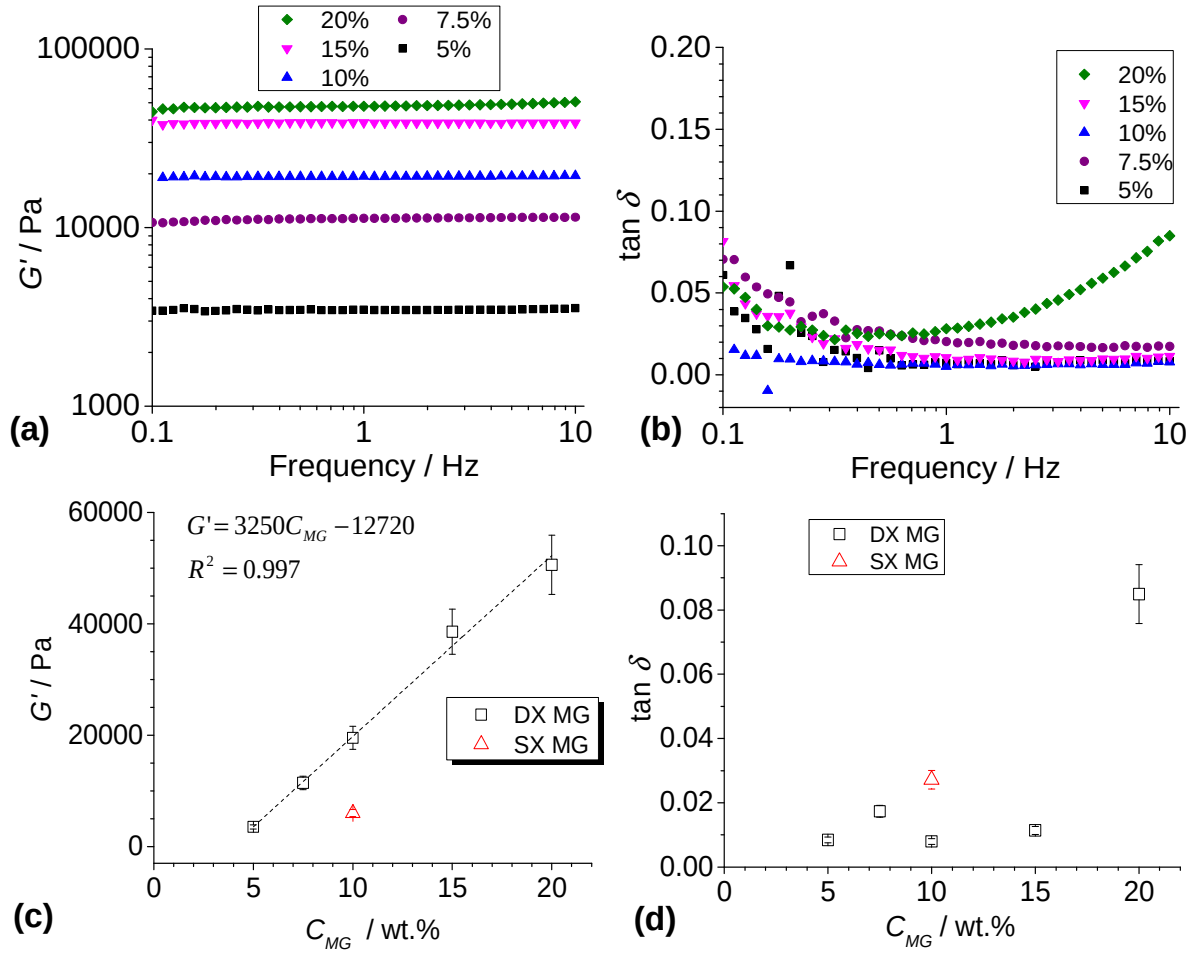

Fig 5. Effect of microgel concentration on P-2 DX MG mechanical properties. (a) and (b) show, respectively, *G'* and tan δ vs. frequency data. (c) and (d) show the dependences of *G'* and tan δ, respectively, on the MG concentration. Data for the non-inter-linked physical gel (SX MG) with y_{exp} = 0 are shown for comparison and are taken from Fig. 6. The *G'* and tan δ values shown were measured at 10 Hz. The error bars were smaller than the data for many of the data points in (d).

The *G'* values measured at 10 Hz were considered plateau values and are plotted as a function of C_{MG} in this study (Fig. 5c). Effective volume fractions occupied by MG particles may be reported for concentrated MG dispersions. Such values are often determined using low concentration

viscosity measurements[32-34]. Extrapolation of those values to higher concentrations often results in effective volume fraction values greater than unity and such values offer limited insight beyond showing that the MG particles have deformed. We therefore used C_{MG} values in this work and note that it is highly likely that the MG particles were deformed in the physical and covalent gels. Interestingly, the *G'* vs. C_{MG} data showed a linear increase with C_{MG} (Fig. 5c). This behaviour contrasts to acrylate-based DX MGs which have been reported to give exponential dependences of *G'* with MG particle concentration[9]. Whilst we cannot be certain of the cause of these differences the linear behaviour observed here may be aided by the very strong swelling nature of the MG particles as evidenced by high *Q* values measured using PCS (Table1). We conjecture that strong MG particle swelling forced the MG peripheries close together and, in turn, favoured efficient inter-MG covalent bonding (Scheme 1).

Fig. 5d shows the tan δ values measured as a function of C_{MG}. Data for the parent non-inter-linked SX MG are also shown at C_{MG} = 10 wt.%. DX MG formation decreased the tan δ value, which has been reported for acrylate based DX MGs[35]. This decrease is attributed to formation of elastically effective linkages between neighbouring particles. The tan δ values are in the range 0.01 to 0.02 for the gels containing C_{MG} < 20 wt.%. These values imply that 98 – 99% of the mechanical energy used to deform the gel matrix was stored for these systems. The tan δ value was significantly larger (0.09 at a frequency of 10 Hz) for the C_{MG} = 20 wt.% system, which suggests a higher proportion of inelastic linkages were present.

In the final part of the study we investigated the effect of vinyl functionalisation on the mechanical properties of the DX MGs using a C_{MG} value of 10 wt. % The latter value was chosen because of the critical behaviour exhibited by P-2 gel discussed above. Fig. 6a shows that the *G'* values were almost frequency independent. This behaviour was also observed for P-0, which was a SX MG physical gel (not doubly crosslinked). Consequently, the low frequency dependence for

the *G'* values is attributed to the close packed nature of the MG particles within the gels (Fig. 4b, c, e and f), rather than the inter-MG linking.

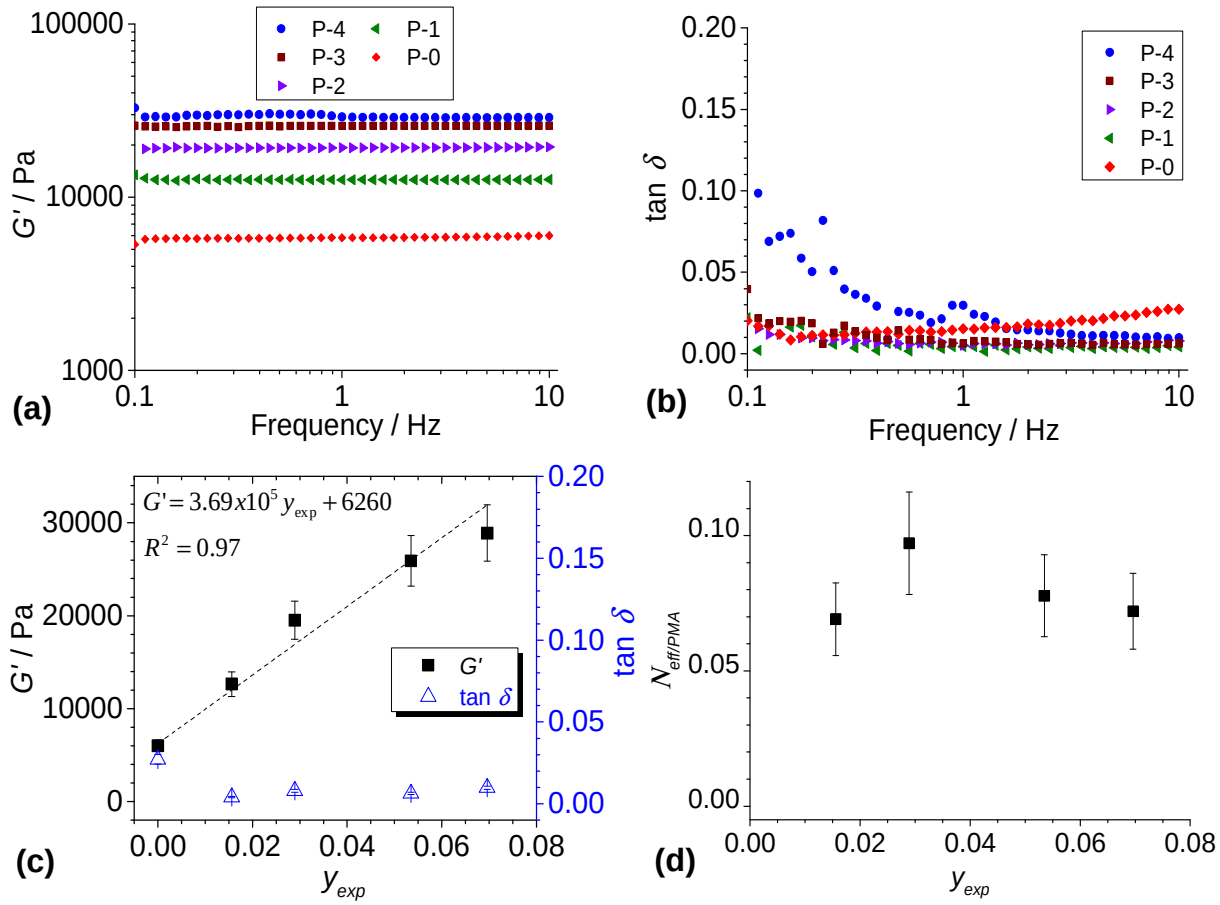

Fig. 6. Effect of extent of vinyl functionalisation on DX MG mechanical properties. (a) and (b) show *G'* and tan δ vs. frequency data, respectively. (c) shows the dependence of *G'* on y_{exp}. Data for tan δ are also plotted. The *G'* and tan δ values shown were obtained at 10 Hz and the DX MG concentration was 10 wt.%. (d) Variation of the calculated number of elastically effective chains per PMA group with y_{exp}.

Low frequency dependences for tan δ were also observed for most of the gels (Fig. 6b). However, the P-0 system (not doubly crosslinked) showed tan δ values that increased with frequency. The P-4 system showed surprisingly high tan δ values which had the same tendency to decrease with increasing frequency that was apparent for most of the other DX MGs. It appears from the data shown in Fig. 5b and 6b that DX MGs which are highly functionalised or have high MG concentrations favour formation of elastically ineffective chains that give rise to frequency dependent tan δ values. Such chains may result from trapping of MG particles in structural arrangements that do not permit sufficient movement for inter-linking to occur.

As shown in Fig. 6c a linear relationship was evident between *G'* and y_{exp}. This result is important for two reasons. It is the first demonstration of the ability to precisely tune the modulus of DX MGs via vinyl functionalisation control. Secondly, the data imply that CuAAC can be used to precisely vary the extent of functionalisation by an azide species within a hydrogel using CuAAC. Part of the reason this approach was successful for the present gels is that the functionalisation occurred with high surface area-to-volume ratio MG particles which were then assembled to form a hydrogel. Uniquely, our DX MG approach means that large scale (slow) diffusion of reactants is not required for uniform functionalisation of a macroscopic hydrogel on the length scale of micrometres. Fig 6c also shows that the tan δ values were only weakly dependent on y_{exp}. The tan δ values were all smaller than that for P-0, which is due to the latter being a SX MG physical gel.

An interesting question that can be addressed using the data presented here concerns the proportion of PMA groups that form elastically effective chains. To address this question we first calculate the number of elastically effective chains per particle ($\nu_{eff(P)}$), then the number of PMA groups per particle ($n_{PMA(P)}$) and finally the number of elastically effective chains per PMA group ($N_{eff/PMA}$). Using the affine approximation the number-density of elastically effective chains (ν_{eff}) is related to the modulus (G) by:

$$G = \upsilon_{eff} kT \quad (2)$$

where k and T are the Boltzmann constant and temperature, respectively. We assume that G and *G'* measured at 10 Hz are equivalent. The *G'* values have contributions from particle-particle interactions and also inter-MG linking. Non-covalent particle-particle interactions were corrected by subtracting the *G'* value for the non-interlinked SX MG physical gel (P-0) from the *G'* values for the DX MGs using the data shown in Fig. 6c. All of the gels had the same C_{MG} value of 10 wt.%. The corrected *G'* values were then used to calculate ν_{eff} from eq. (2) - See Table 2.

Table 2. Estimation of the number of elastically effective chains per PMA unit.

Code	M_p[a] / 10^{-14} g	ν_{eff}[b] / 10^{24} m^{-3}	$\nu_{eff(P)}$[c] / 10^5	$n_{PMA(P)}$[d] / 10^6	$N_{eff/PMA}$[e]
P-0	1.6	-	-	-	-
P-1	1.4	1.6	2.3	3.3	0.069
P-2	1.8	3.3	5.9	6.1	0.097
P-3	1.8	4.8	8.7	11	0.078
P-4	1.9	5.6	10	15	0.070

[a] Particle mass. [b] Number density of elastically effective chains. [c] Number of elastically effective chains per particle. [d] Number of PMA groups per particle. [e] Number of elastically effective chains per PMA group.

Calculation of the value for $\nu_{eff(P)}$ required the mass of a particle (M_P) which was calculated from the diameters of the collapsed particles obtained from SEM (Table 1). The M_P and $\nu_{eff(P)}$ values appear in Table 2. The $\nu_{eff(P)}$ values are of the order of 10^5 to 10^6, and are comparable to those calculated by Roeder et al.[36] for their vinyl-functionalised hematite particle gels. To calculate the value for $n_{PMA(P)}$ we used the composition of the parent P-0 particles as well as the particle mass to estimate the number of PA molecules per particle. Use of the y_{exp} values (Table 1) then enabled calculation of $n_{PMA(P)}$ (Table 2). $N_{eff/PMA}$ values were calculated from the ratios of $\nu_{eff(P)}$ to $n_{PMA(P)}$ (Table 2) and are plotted in Fig. 6d.

The data shown in Fig. 6d provide an estimate of the proportion of vinyl groups that are involved in DX MG formation for the first time. The average value for $N_{eff/PMA}$ was 0.080 (i.e., 8 %) and there was no significant difference for the gels (Fig. 6d). The relatively low proportion of PMA groups that formed elastically effective chains is reasonable for two reasons. Firstly, the PMA groups were probably distributed throughout each MG particle. Secondly, the elastically effective chains result from inter-MG linking at the particle peripheries. Hence, a low proportion of PMA groups will be available for inter-MG linking because most of the PMA groups would have resided within the MG interior. Furthermore, because $N_{eff/PMA}$ appears to be constant it follows that using our approach and CuAAC it is possible to precisely tune the number of inter-linking

reactants at the surfaces of MG particles. The DX MG approach combined with CuAAC provides a remarkable ability to precisely control, and even "dial up", ν_{eff} and hydrogel modulus through construction of pre-formed MG building blocks.

Conclusions

In this study we have used CuAAC to vinyl functionalise cationic PVP-PA MG particles and create new DX MGs using a synthetic method that did not compromise colloidal stability. CuAAC efficiencies were calculated to be in the range of 79 to 96% and enabled precise control of the vinyl functionalisation over the range of 0 to 7.0 mol.% The mechanical properties were probed by dynamic rheology and the modulus varied linearly with C_{MG} over the range of about 11 to 51 kPa. Furthermore, the modulus also varied linearly with y_{exp} over the range of 13 to 29 kPa for DX MGs prepared C_{MG} = 10 wt.% Analysis of the data revealed that ~ 8 % of the PMA groups formed elastically effective chains and this appeared to be independent of y_{exp}. The former value was attributed to the location of the PMA groups at the periphery of the MG particles being key to DX MG formation. The study presented here provides the first example of a VP-based DX MG and also demonstrates the ability of CuAAC to enable unprecedented control of hydrogel functionalisation. Not only does this work pave the way for improvements in hydrogel functionalisation and also new tools for precisely "dialing up" gel modulus but it should also increase the number of gels that can be prepared by the DX MG route. This expansion in the number of DX MG types should be possible by inclusion of PA during MG synthesis and utilisation of our CuAAC approach. Furthermore, the presence of latent functionality of the unreacted acetylene groups in the MG particles (Scheme 1) offers excellent potential for additional functionalisation of the MG particles prior to DX MG formation, which could enable construction of next generation functional hydrogels. Future control of the ordering of the MG particles within VP-based DX MGs may also provide a new generation of photonic gels as well as membranes.

Acknowledgements

We would like to thank the EPSRC for funding RF through a DTA scholarship.

References

1. J. P. Gong. *Soft Matter* 2010, **6**, 2583-2590.
2. K. Haraguchi, and T. Takehisa. *Adv. Mater.* 2002, **14**, 1120-1124.
3. T. Sakai, T. Matsunaga, Y. Yamamoto, C. Ito, R. Yoshida, S. Suzuki, N. Sasaki, M. Shibayama, and U.-I. Chung. *Macromolecules* 2008, **41**, 5379-5384.
4. K. Oshima, T. Fujimoto, E. Minami, and Y. Mitsukami. *Macromolecules* 2014, **47**, 7573-7580.
5. A. Argun, V. Can, U. Altun, and O. Okay. *Macromolecules* 2014, **47**, 6430-6440.
6. S. Chatani, C. Wang, M. Podgórski, and C. N. Bowman. *Macromolecules* 2014, **47**, 4949-4954.
7. Z. P. Demko, and K. B. Sharpless. *Angew Chem Int Ed Eng* 2002, **41**, 2113-2116.
8. R. K. Iha, K. L. Wooley, A. M. Nyström, D. J. Burke, M. J. Kade, and C. J. Hawker. *Chem. Rev.* 2009, **109**, 5620-5686.
9. R. Liu, A. H. Milani, T. J. Freemont, and B. R. Saunders. *Soft Matter* 2011, **7**, 4696-4696.
10. B. R. Saunders, and B. Vincent. *Adv. Coll. Interf. Sci.* 1999, 1-25.
11. W. Richtering, and B. R. Saunders. *Soft Matter* 2014, **10**, 3695-3702.
12. S. Thaiboonrod, A. H. Milani, and B. R. Saunders. *J. Mater. Chem. B* 2014, **2**, 110-119.
13. R. Farley, and B. R. Saunders. *Polymer* 2014, **55**, 471-480.
14. J. A. Burdick, and W. L. Murphy. *Nature Commun.* 2012, **3**, 1269-1277.
15. W. E. Hennink, and C. F. van Nostrum. *Adv. Drug Deliv. Rev.* 2012, **64**, 223-236.
16. D. Dupin, S. Fujii, S. P. Armes, P. Reeve, and S. M. Baxter. *Langmuir : the ACS journal of surfaces and colloids* 2006, **22**, 3381-3387.
17. A. Loxley, and B. Vincent. *Colloid and polymer science* 1997, **275**, 1108-1114.
18. J. McParlane, D. Dupin, J. M. Saunders, S. Lally, S. P. Armes, and B. R. Saunders. *Soft Matter* 2012, **8**, 6239-6239.
19. W. D. Sharpless, and J. G. Lindberg. 2005, **82**, 1833-1836.
20. M. T. Gokmen, and F. E. Du Prez. *Prog. Polym. Sci.* 2012, **37**, 365-405.
21. X. Jiang, E. B. Vogel, M. R. S. Iii, and G. L. Baker. *Macromolecules* 2008, 1937-1944.
22. M. Malkoch, R. Vestberg, N. Gupta, L. Mespouille, P. Dubois, A. F. Mason, J. L. Hedrick, Q. Liao, C. W. Frank, K. Kingsbury, and C. J. Hawker. *Chem. Comm.* 2006, 2774-2776.
23. S. G. Kupal, B. Cerroni, S. V. Ghugare, E. Chiessi, and G. Paradossi. *Biomacromolecules* 2012, **13**, 3592-3601.
24. Z. Meng, G. R. Hendrickson, and L. A. Lyon. *Macromolecules* 2009, **42**, 7664-7669.
25. B. S. Sumerlin, N. V. Tsarevsky, G. Louche, R. Y. Lee, and K. Matyjaszewski. *Macromolecules* 2005, **38**, 7540-7545.
26. D. J. Shaw (1992) *Introduction to colloid and surface chemistry*, Butterworth-Heinemann Ltd., Oxford.
27. A. S. Lang, A. Neubig, M. Sommer, and M. Thelakkat. *Macromolecules* 2010, **43**, 7001-7010.
28. X. Li, X. Wei, and S. M. Husson. *Biomacromolecules* 2004, **5**, 869-876.
29. H. Ohshima. *Current Opinion in Colloid & Interface Science* 2013, **18**, 73-82.
30. T. Lane, J. L. Holloway, A. H. Milani, J. M. Saunders, A. J. Freemont, and B. R. Saunders. *Soft Matter* 2013, **9**, 7934-7941.
31. H. H. Winter, and F. Chambon. *J. Rheol.* 1986, **30**, 367-382.
32. L. A. Lyon, J. D. Debord, S. B. Debord, C. D. Jones, J. G. McGrath, and M. J. Serpe. *J. Phys. Chem. B* 2004, **108**, 19099-19108.
33. H. Senff, and W. Richtering. *J. Chem. Phys.* 1999, **111**, 1705-1711.
34. K. Urayama, T. Saeki, S. Cong, S. Uratani, T. Takigawa, M. Murai, and D. Suzuki. *Soft Matter* 2014,

10, 9486-9495.

35. R. Liu, A. H. Milani, J. M. Saunders, T. J. Freemont, and B. R. Saunders. *Soft Matter* 2011, **7**, 9297-9297.
36. L. Roeder, M. Reckenthäler, L. Belkoura, S. Roitsch, R. Strey, and A. M. Schmidt. *Macromolecules* 2014, **47**, 7200-7207.